American Psychological Association

Journal of Comparative Psychology

© 2019 American Psychological Association
0735-7036/19/$12.00

2019, Vol. 133, No. 2, 143–155
http://dx.doi.org/10.1037/com0000172

Local Interaction Rules and Collective Motion in Black Neon Tetra (*Hyphessobrycon herbertaxelrodi*) and Zebrafish (*Danio rerio*)

Vicenç Quera, Elisabet Gimeno, Francesc S. Beltran, and Ruth Dolado
University of Barcelona

We explored the local motion rules used by interacting individuals in small groups of black neon tetra (*Hyphessobrycon herbertaxelrodi*) and zebrafish (*Danio rerio*) to ascertain if and how these rules underlie the fishes' global collective coordinated motion. As these 2 species show very different styles of collective motion in terms of cohesion and polarization, we expected to find differences in their individual behavioral rules. We recorded groups of 2, 3, 4, and 8 fish of each species; tracked their individual trajectories; and studied how their individual turning angles and accelerations varied as a function of heading differences, distances, and relative angles to their neighbors. We found that black neon tetra and zebrafish differed in terms of their preferential positions with respect to their neighbors, the magnitude of turning angles and accelerations, and the way these angles and accelerations are modulated by both the distance from neighbors (thus suggesting a "repulsion" zone in black neon tetra but not in zebrafish) and the heading difference and relative angle to neighbors. Our results enable us to infer that, in black neon tetra, avoiding excessive proximity and collision takes priority over cohesion, and cohesion takes priority over polarization. This provides evidence that rules are similar in species of very different genera and that differences are a matter of degree. Our results also provide substantial empirical evidence to support the theoretical assumptions made in agent-based models that simulate coordinated collective motion in many different animal species.

Keywords: coordinated collective motion, local interaction rules, *Hyphessobrycon herbertaxelrodi*, *Danio rerio*

This document is copyrighted by the American Psychological Association or one of its allied publishers.
This article is intended solely for the personal use of the individual user and is not to be disseminated broadly.

Crowds of people (Helbing, Molnár, Farkas, & Bolay, 2001), flocks of birds (Emlen, 1952; Nagy, Ákos, Biro, & Vicsek, 2010), herds of mammals (Gueron, Levin, & Rubenstein, 1996; King & Sueur, 2011), shoals and schools of fish (Couzin, James, Mawdsley, Croft, & Krause, 2006; Pitcher & Parrish, 1993; Radakov, 1973), and swarms of insects (Buhl et al., 2006; Deneubourg & Goss, 1989) are natural phenomena that share a common feature: through local interactions, individuals in the group synchronize their movements and achieve large-scale, coordinated collective motion (CCM). Exhaustive research has been done on the topic in recent years (for a review, see Vicsek & Zafeiris, 2012), and both empirical and simulation data have been obtained. To study CCM empirically, it is necessary to record the simultaneous movements of a great number of individuals (i.e., their positions and trajectories over time), and this process involves major technical difficulties (Delcourt, Denoel, Ylieff, & Poncin, 2013).

Computer simulation is therefore a common approach to the study of CCM and includes the use of agent-based models (Kunz & Hemelrijk, 2003; Quera, Beltran, & Gimeno, 2016), which implement local interaction rules that lead to the emergence of global motion like that observed in nature. Although some empirical findings in real organisms match the findings obtained in simulation (e.g., by varying the perceptual depth of virtual fish, they tend to achieve a degree of coordination very much like that of real fish under different levels of environmental luminosity and water visibility; Quera et al., 2016), it still remains unclear whether the rules implemented in the models fit the rules that the organisms actually follow, because many collective motion patterns observed in nature can be simulated by models that use very different interaction rules. For example, regarding the models proposed for CCM in fish, a common assumption is that individuals move according to rules of attraction to and repulsion from their immediate neighbors and that they align (or polarize) with respect to them by adjusting their headings and velocities (Aoki, 1982; Couzin, Krause, James, Ruxton, & Franks, 2002; Huth & Wissel, 1994; Reynolds, 1987).

However, empirical studies on CCM in fish have found no evidence that they actually try to match their headings and have concluded that polarization is likely to be an emergent phenomenon (Herbert-Read et al., 2011; Katz, Tunstrøm, Ioannou, Huepe, & Couzin, 2011). Likewise, although some models assume that only one alignment rule is necessary to achieve CCM (Czirók &

This article was published Online First February 25, 2019.

Vicenç Quera, Elisabet Gimeno, Francesc S. Beltran, and Ruth Dolado, Institute of Neurosciences (NeuroUB), Quantitative Psychology Unit, University of Barcelona.

This project was supported by grants from the Ministerio de Economía, Industria y Competitividad of Spain (PSI2012-32007, PSI2015-63743-P, and BES-2013-063615).

Supplemental videos are available from the Open Science Framework: https://osf.io/5n9e2/.

Correspondence concerning this article should be addressed to Vicenç Quera, Quantitative Psychology Unit, University of Barcelona, Campus Mundet, Passeig Vall d'Hebron, 171, 08035 Barcelona, Spain. E-mail: vquera@ub.edu

This document is copyrighted by the American Psychological Association or one of its allied publishers.
This article is intended solely for the personal use of the individual user and is not to be disseminated broadly.

Vicsek, 2000), others show that such a rule is not necessary and that preferential positioning in relation to neighbors (Perna, Grégoire, & Mann, 2014; Quera et al., 2016) or attraction to them (Strömbom, 2011) is sufficient to make CCM emerge.

Therefore, regarding CCM in shoals and schools of fish, it seems reasonable to explore the local interaction rules actually applied by real individuals and try to determine if and how these rules are responsible for global coordinated motion. Without this information, it is difficult to select plausible models based only on the fit between the global group measures they predict (e.g., mean interindividual distances or polarization; Delcourt & Poncin, 2013) and empirical ones, given that models with different interaction rules tend to yield very similar global outcomes (Vicsek & Zafeiris, 2012). Several empirical studies of fish (mosquitofish, *Gambusia holbrooki*, and golden shiners, *Notemigonus crysoleucas*) have been published in the past 10 years showing that a set of local interaction rules on the relative position of the individuals and their acceleration and turning angles, among other measures, may explain the CCM observed (Herbert-Read et al., 2011; Katz et al., 2011; Rosenthal, Twomey, Hartnett, Wu, & Couzin, 2015).

Social groups of fish show different types of CCM. If the individuals show a significant degree of cohesion (i.e., they tend to remain close to each other), then the CCM is labeled a *shoal*, and if the individuals move synchronically, with a similar velocity and alignment, then the CCM is labeled a *school* (Pitcher & Parrish, 1993). Therefore, a key concept for differentiating between a shoal and a school is group polarization, a global measure of group coordination that describes individuals' tendency to adopt the same orientation as their group mates (Delcourt & Poncin, 2013).

Some comparative studies have explored the differences in the CCM of different fish species (Leem, Jeon, Yun, & Lee, 2012; Soria, Fréon, & Chabanet, 2007). Gimeno, Quera, Beltran, and Dolado (2016) compared the CCM of zebrafish (*Danio rerio*) and black neon tetra (*Hyphessobrycon herbertaxelrodi*) and found that the two species had different types of CCM, given that the global motion of zebrafish matched that of a *shoal* and the global motion of black neon tetra matched that of a *school*. It seems reasonable to assume that different individual behavioral rules may underlie different global motion styles. We analyzed the movements of individuals in groups of zebrafish and black neon tetra to determine the local interaction rules from which different global CCM patterns can arise. Moreover, as there is evidence that group size has an effect on CCM in fish (Calovi, Lopez, Ngo, Sire, Chaté, & Theraulaz, 2014; Shelton, Price, Ocasio, & Martins, 2015; Soria et al., 2007), we explored local interaction rules with different group sizes (N = 2, 3, 4, and 8). We expected to find differences in the local interaction rules of the two species studied, as well as differences across group sizes.

Method

Subjects

Thirty-four adult wild-type fishes were used in the experiment, 17 zebrafish (*Danio rerio*; mean body length: 3 cm) and 17 black neon tetra (*Hyphessobrycon herbertaxelrodi*; mean body length: 2.5 cm). Although zebrafish and black neon tetra have different body lengths, their fusiform shapes are very similar.

They were obtained from a local vendor (Corallus, Gavà, Barcelona). Before beginning the experiment, they were acclimated to our facilities for a minimum of 2 months. Initially, 30 black neon tetra and 30 zebrafish were kept in two separate main aquaria measuring 40 × 43 × 30 cm. For each species, 17 fish were randomly selected and assigned to the four different groups (two, three, four, and eight subjects); each group was housed in a smaller experimental aquarium (20 × 14 × 14 cm for the groups of two, three, and four individuals, and 34 × 20 × 22 cm for the groups of eight individuals) 1 week before the experiments started and while the experiment lasted. Both the main and the experimental aquaria were maintained on a regular light/dark cycle, water temperature was maintained at 25 ± 2 °C (main aquaria) and 21–22 °C (experimental aquaria), pH at 7.8–8, total hardness at 8–14° dH, and carbonated hardness at 8–14° dH. Ammonium and nitrite concentrations were nil, whereas nitrate levels were below 50 mg/L. Water quality was kept optimal by performing weekly 15% water changes. Fishes were fed to satiation on Ocean Nutrition Community Formula Flakes (Ocean Nutrition Europe, Belgium). Applicable institutional guidelines for the care and use of animals were followed. All procedures performed were in accordance with the standards approved by the Ethics Committee of the University of Barcelona at which the studies were conducted.

Apparatus

The experimental tank was 100 × 93 × 40 cm (see Figure 1), and the water column height was 15 cm. The tank was indirectly lit by six lamps surrounding it, which provided homogeneous, low-intensity light. Videos were recorded with a digital camera (uEye UI-1640LE) mounted 2.2 m above the center of the tank. The camera was linked to a computer (HP Z420, Intel Xeon E5-1620), and the signal was recorded using the uEye Cockpit software program (IDS, Imaging Development Systems GmbH, https://es.ids-imaging.com). Videos were recorded at 20 fps, 8-bit gray, and a resolution of 1176 × 1016 pixels, which corresponds to the area occupied by the tank.

Procedure

Each experimental group (of two, three, four, and eight individuals) was video-recorded daily for 5 min. The procedure was replicated first for 10 days with the zebrafish, then for 10 days with the black neon tetra. To ensure the fishes became acclimatized to the temperature in the experimental tank (25 °C), prior to the recording session, each group was transferred from its experimen-

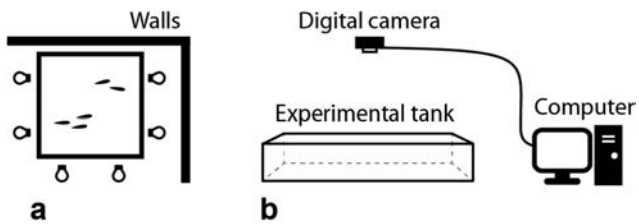


Figure 1. Schematic representation of the experimental setup. a) Top view of the tank and position of the lights (23 W). All lights face away from the experimental tank. b) A digital camera above the experimental tank sends a digital signal to a computer, which records the videos.

tal aquarium into a bucket containing a mixture of water from the experimental tank and the fishes' aquarium and remained there for 5 min. The fishes were then transferred into the experimental tank. After another 5 min of habituation to the new environment, we recorded their activity for 5 min. For each recording session, we took a snapshot of the experimental tank before the fishes were transferred and later used that snapshot for background subtraction when the videos were analyzed. Once the recording was made, the fishes were captured with a net and transferred back to their experimental aquarium, to which water from the experimental tank was added to facilitate reacclimatization. At the end of the daily recording sessions, water was added to the experimental tank to compensate for the water transferred into the experimental aquaria.

As the four groups of each species were used in succession each day, the order in which they were recorded was randomly sorted daily to control for possible cumulative effects of the decrease in water temperature (because the heaters were removed from the experimental tank during recording) and any pheromones or chemical signals left in the water by the preceding group. Eighty videos were recorded with a total of 6 h 40 min of footage. Video fragments were decomposed into frames using VirtualDub 1.19.11 (Lee, 2013), and a stack of 6,000 frames per fragment was obtained. We randomly selected six packs of 500 consecutive frames for each fragment, resulting in six replicas of 25 s per group and day, that is, 60 replicas per group. In total, 1 h 40 min of footage (120,000 frames) was analyzed per species. Using ImageJ (Rasband, 2014), each pack of images was segmented by subtracting the background, and then a method to resolve occlusions was applied to the binary images, in which fishes were represented as black objects against a white background. Occlusions occurred when two or more individuals swam too close together, causing them to be represented as a single object. We applied a set of ImageJ macros to resolve occlusions automatically; the method is described in the work by Dolado, Gimeno, Beltran, Quera, and Pertusa (2015). Any occlusions that could not be resolved automatically using the method were manually split by a trained observer using ImageJ. Finally, the stacks of occlusion-free frames were compiled into video files and analyzed with multitracking software Image-Pro Premier 9.1 (Media Cybernetics, Inc., 2015) to acquire the individual fish trajectories in two dimensions. The resulting trajectories were checked by an observer, and any erroneous identity assignments made by the motion prediction model of software Image-Pro Premier 9.1 were manually corrected. Supplemental videos are available from the Open Science Framework (https://osf.io/5n9e2/). The trajectory files were then processed using R scripts (R Development Core Team, 2014); first, we smoothed the fish coordinates using the moving average method with a time window of seven frames (0.35 s) to remove any inaccuracies caused by the tracking and occlusion resolving methods, and then we computed the distances, heading differences, and relative positions of each pair of individuals at each video frame. Dyadic interactions were analyzed by exploring how these variables were associated to fish accelerations and turning angles.

Measures

Interindividual distance. Given the pixel coordinates at frame t of fish i, $[x_i(t), y_i(t)]$, and fish j, $[x_j(t), y_j(t)]$, the Euclidean distance between them is:

$$d_{ij}(t) = ([x_i(t) - x_j(t)]^2 + [y_i(t) - y_j(t)]^2)^{1/2}$$

The average distance among all pairs of N individuals at frame t is a global measure of the group's cohesive tendency; the smaller the average distance, the more cohesive the group (Miller & Gerlai, 2012b):

$$\bar{d}(t) = \frac{2}{N(N-1)} \sum_{i=1}^{N-1} \sum_{j=i+1}^{N} d_{ij}(t)$$

Comparing interindividual distances in species with different body lengths involves calculating the ratio of average distance to mean body length ($\bar{L}$; Delcourt & Poncin, 2013):

$$D(t) = \frac{\bar{d}(t)}{\bar{L}}$$

Polarization. This global measure quantifies the degree of alignment among a group of fish at frame t and is calculated as the module of the mean heading vector of all individuals (Miller & Gerlai, 2012a):

$$P(t) = \frac{1}{N} \left| \sum_{i=1}^{N} \boldsymbol{h}_i(t) \right|$$

where $\boldsymbol{h}_i(t)$ is the heading of fish i. The vector linking its position at frame $t-1$ to that at frame t is its velocity, $\boldsymbol{v}_i(t) = [x_i(t) - \boldsymbol{x}_i(t-1), y_i(t) - y_i(t-1)]$, and:

$$\boldsymbol{h}_i(t) = \frac{\boldsymbol{v}_i(t)}{|\boldsymbol{v}_i(t)|}$$

Polarization has values in the range [0, 1]; when all the individuals are perfectly aligned, it equals 1, and when the individuals' heading vectors cancel each other, it equals 0.

Heading difference. The heading difference $\gamma_{ij}(t)$ from fish i to fish j at frame t is the angle from $\boldsymbol{h}_i(t)$ to $\boldsymbol{h}_j(t)$:

$$\gamma_{ij}(t) = \cos^{-1}[\boldsymbol{h}_i(t) \cdot \boldsymbol{h}_j(t)]$$

Heading differences have values in the range $[-180°, +180°]$. The sign of $\gamma_{ij}(t)$ is that of the vector product $\boldsymbol{h}_i(t) \times \boldsymbol{h}_j(t)$, that is, positive angles mean "left," or counterclockwise, negative angles mean "right," or clockwise, and null angles indicate that the headings are parallel (the fish are polarized).

Relative angle. The relative angle $\alpha_{ij}(t)$ from fish i to fish j at frame t is the angle from $\boldsymbol{h}_i(t)$ to the unit vector that points from i's to j's position, $\boldsymbol{e}_{ij}(t)$:

$$\alpha_{ij}(t) = \cos^{-1}[\boldsymbol{h}_i(t) \cdot \boldsymbol{e}_{ij}(t)]$$

Again, the sign of $\alpha_{ij}(t)$ is that of the vector product $\boldsymbol{h}_i(t) \times \boldsymbol{e}_{ij}(t)$, that is, $\alpha_{ij} > 0°$ means that j is to the left of i; $\alpha_{ij} < 0°$ means that j is to the right of i; $\alpha_{ij} = 0°$ means that j is in front i; and $\alpha_{ij} = \pm 180°$ means that j is behind i. Conversely, the relative angle from j to i at frame t is $\alpha_{ji}(t) = \cos^{-1}[\boldsymbol{h}_j(t) \cdot \boldsymbol{e}_{ji}(t)]$, where $\boldsymbol{e}_{ji}(t)$ is the unit vector that points from j's to i's position, and its sign is that of the vector product $\boldsymbol{h}_j(t) \times \boldsymbol{e}_{ji}(t)$. It should be noted that the relative angles and heading difference between two fish are related:

$$\alpha_{ji}(t) = \alpha_{ij}(t) - \gamma_{ij}(t) + k$$

where $k = +180°$ when $\alpha_{ij}(t) \leq \gamma_{ij}(t)$ and $k = -180°$ when $\alpha_{ij}(t) > \gamma_{ij}(t)$.

This document is copyrighted by the American Psychological Association or one of its allied publishers.
This article is intended solely for the personal use of the individual user and is not to be disseminated broadly.

Turning angle. The turning angle $\beta_i(t)$ of a fish at t, the angle from its previous heading to its current one, is:

$$\beta_i(t) = \cos^{-1}[\boldsymbol{h}_i(t-1) \cdot \boldsymbol{h}_i(t)]$$

Turning angles have values in the range $[-180°, +180°]$, their sign is that of the vector product $\boldsymbol{h}_i(t-1) \times \boldsymbol{h}_i(t)$, and they are expressed in degrees/frame. The sign of $\beta_i(t)$ indicates a left ($\beta_i > 0°$) or right ($\beta_i < 0°$) turn. Schematic representations of these measures are shown in Figure 2.

Acceleration. Given the velocities of fish i at video frames t and $t-1$, its acceleration at t is computed as the difference between the module of its velocity at t minus that at $t-1$ and is expressed in pixels/frame^2:

$$s_i(t) = |\boldsymbol{v}_i(t)| - |\boldsymbol{v}_i(t-1)|$$

Units of measurement. As the dimensions of the experimental tank were 100 × 93 cm and the video resolution was 1176 × 1016 pixels, distances in pixels were converted into distances in centimeters by multiplying them by $\frac{1}{2}\left(\frac{100}{1176} + \frac{93}{1106}\right) = .0846$. As the time resolution was .05 s/frame, accelerations (in pixels/frame^2) and turning angles (in degrees/frame) were converted into cm/s^2 and degrees/s by multiplying them by $.0846/.05^2 = 33.84$ and .05, respectively.

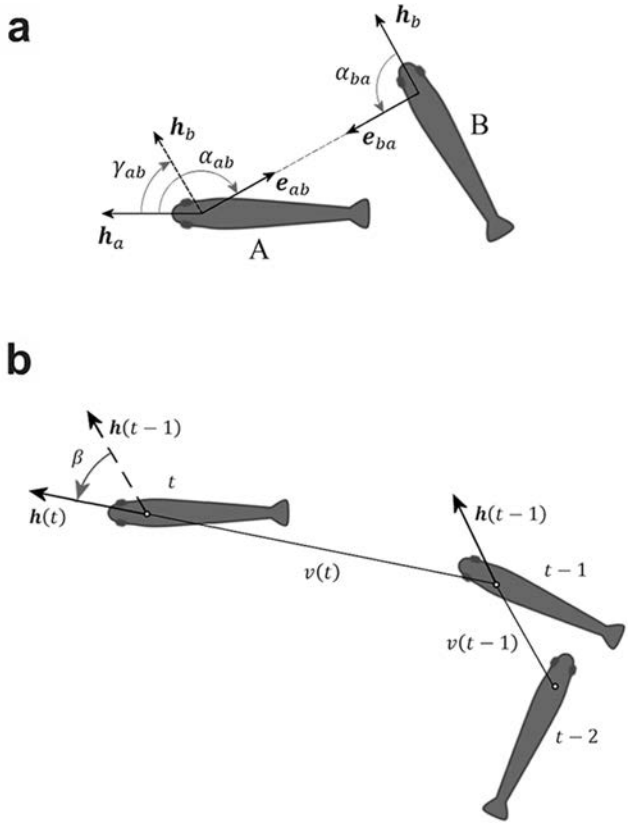


Figure 2. Measures used to analyze local interaction between two fish. a) Measures at frame t for focal fish A relative to neighbor B: $\boldsymbol{h}_a$ and $\boldsymbol{h}_b$, headings; γ_{ab}, heading difference from A to B; α_{ab}, relative angle from A to B; α_{ba}, relative angle from B to A. b) Movement of focal fish: $v(t)$ and $v(t-1)$, velocities; β, turning angle.

Results

Figure 3 shows the results for the global measures of collective motion of the fishes as a function of group size and species. Both the ratio of mean interindividual distance to mean body length (D) and polarization (P) were averaged for each video fragment (see Table 1). A two-way analysis of variance indicated that the D ratio was significantly different between group sizes, $F(3, 472) = 25.32$, $p < .001$, $\eta^2 = 0.139$, and between species, $F(1, 472) = 5.47$, $p < .020$, $\eta^2 = 0.01$; no significant interaction between the two variables was found. Black neon tetra were generally more cohesive than zebrafish, and small groups were more cohesive than big ones (differences were significant except for those for sizes 3 and 4; see Figure 3a). Regarding polarization, a two-way analysis of variance showed that the differences were significant between group sizes, $F(3, 472) = 99.11$, $p < .001$, $\eta^2 = 0.386$, and between species, $F(1, 472) = 768.51$, $p < .001$, $\eta^2 = 0.62$, with significant interaction between these variables, $F(3, 472) = 41.98$, $p < .001$, $\eta^2 = 0.211$. Globally, black neon tetra were more polarized than zebrafish. Although the bigger group sizes showed less polarization, the decrease was significantly greater for zebrafish; differences were significant except for those for sizes 3 and 8 (black neon tetra) and 4 and 8 (zebrafish; see Figure 3b). Correlation between polarization and mean interindividual distance was negative but weak. In black neon tetra, $r = -.198$, $p = .002$; in zebrafish, $r = -.340$, $p < .001$; in both cases, $n = 240$ replicas, pooled over group size.

Figure 4 shows circular histograms of heading differences (γ) and relative angles (α) as a function of species and group size; these measures were computed for each individual taken as focal and aggregated for all individuals. The focal fish is located at the center of the diagrams facing 0°. In the histograms of heading differences, high frequencies for angles close to zero and low ones for angles far from zero indicate that the headings of neighbor fish tend to be like that of the focal fish, that is, pairs tend to be highly polarized. For all group sizes, black neon tetra were more polarized than zebrafish, in accordance with the global results presented above. In the histograms of relative angles, high frequencies for angles close to 0° and 180° and low frequencies for other angles indicate that neighbors tend to be located in front of (0°) or behind (180°) the focal fish. In zebrafish, for all group sizes, the distributions are clearly bimodal, indicating that neighbors tend to be located both in front and behind the focal fish rather than alongside it. In black neon tetra, the distributions are more uniform, indicating that there are no preferential positions.

Figure 5 shows the average turning angle of focal fish as a function of the relative angle to its neighbor, pooled over group size. Maximum mean left turn angles are $\beta_a = +20.04°$ (neon) and $\beta_a = +94.35°$ (zebrafish) when α_{ab} is close to $+90°$ (i.e., turn left when neighbor is on the left) and maximum mean right turn angles are $\beta_a = -20.98°$ (neon) and $\beta_a = -90.22°$ (zebrafish) when α_{ab} is close to $-90°$ (i.e., turn right when neighbor is on the right). In both species, mean turn angles are close to zero when either $\alpha_{ab} = 0°$ (the neighbor is in front) or $\alpha_{ab} = 180°$ (the neighbor is behind).

However, in both species, the tendency of fish to turn depends on not only the relative angle to their neighbors but also the heading difference between them. The tendency to turn is greater in zebrafish than in black neon tetra, as the scales for the heat maps in Figure 6 indicate. As Figure 6a shows, when a neighbor is on the

This document is copyrighted by the American Psychological Association or one of its allied publishers.
This article is intended solely for the personal use of the individual user and is not to be disseminated broadly.

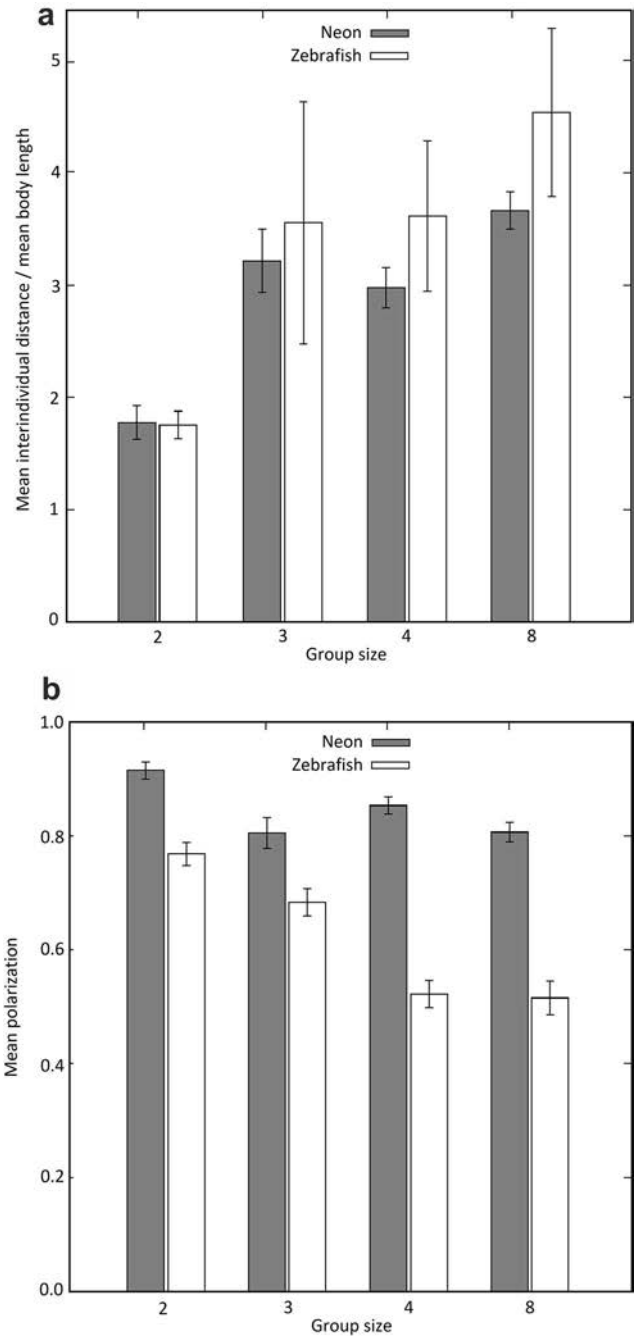


Figure 3. Global measures of collective motion as a function of group size in black neon tetra and zebrafish. a) Ratio of mean interindividual distance to mean body length of the species. b) Mean polarization. Means for 60 replications. Error bars indicate 95% confidence intervals.

left ($\alpha_{ab} > 0°$), turns are mainly to the left (light areas, $\beta_a > 0°$), and when it is on the right ($\alpha_{ab} < 0°$), turns are mainly to the right (dark areas, $\beta_a < 0°$). The heading difference modulates the magnitude of turn, which is high when γ_{ab} is close to $\pm 90°$ and low when it is close to 0° (i.e., when the focal and neighbor fish are polarized). This result is found in both black neon tetra and zebrafish, and for all group sizes, and becomes clearer as group size increases. For black neon tetra, the magnitude of turn of the focal fish tends to be higher when the relative angle and heading difference to its neighbor have opposite signs, that is, when the neighbor is oriented toward the focal fish (α_{ba} is close to 0°), than when they have the same sign, that is, when the neighbor is oriented away from the focal fish (α_{ba} is close to 180°). This effect is not so evident in zebrafish, where the magnitude of turn does not seem to depend on whether the neighbor is oriented toward or away from the focal fish; also, the effect is consistent across group size, although it is not so clear for black neon tetra with $N = 2$.

Turning angles are also dependent on the distance between the focal fish and its neighbor (Figure 6b). For the range of distances explored (up to 200 pixels, 16.92 cm), the greater the distance, the higher the turning angle. Also, turning angles tend to be maximum when the relative angle α_{ab} is close to, but lower than, $\pm 90°$. This result is consistent across species and group size, even with scarce data for $N = 2$. In black neon tetra, at short distances (0 to 5 cm), the sign of the turning angle is reversed: when the neighbor is at less than 5 cm and on the left, the focal fish tends to turn right, and when it is on the right, the focal fish tends to turn left. That is, short distances tend to provoke "repulsion," probably to avoid collision, whereas longer distances tend to provoke "attraction." No such result is seen in the zebrafish data in Figure 6b.

Like turning angles, accelerations and decelerations are higher in zebrafish than in black neon tetra, as Figure 7a shows. Maximum mean acceleration occurs when the relative angle from the focal fish to its neighbor is $\alpha_{ab} = 0°$ (the neighbor is in front): $s_a = 3.36$ cm/s^2 (neon) and $s_a = 4.84$ cm/s^2 (zebrafish); maximum mean deceleration occurs when $\alpha_{ab} = \pm 180°$ (the neighbor is behind): $s_a = -2.83$ cm/s^2 (neon) and $s_a = -3.37$ cm/s^2 (zebrafish). Acceleration is a function of the distance between the focal and neighbor fish. When the neighbor fish is in front and at a distance greater than roughly the species body length, the focal accelerates; the greater the distance between them, the more it accelerates. Conversely, when the neighbor is behind, the focal decelerates, and the greater the distance between them, the more it decelerates (Figure 7b).

Acceleration depends on the heading difference between the fish as well. As Figure 8a shows, in both species, acceleration is high when neighbor fish are in front (α_{ab} is close to 0°) and their headings are nearly opposite to that of the focal fish (γ_{ab} is close to $\pm 180°$), that is, when the fish are facing each other and, according to the results in Figure 7b, when they are far away from each other. Weak acceleration can be detected when neighbor fish are in front of the focal one and are polarized (γ_{ab} is close to 0°), especially in zebrafish for group sizes 4 and 8. On the other hand, in black neon tetra, deceleration is high when they are polarized and the neighbor fish are not in front of the focal fish (γ_{ab} is close to 0° and $|\alpha_{ab}| \geq 90°$) and, again, when they are far away from each other. Average accelerations as a function of distance, relative angle, group size, and species, are shown in Figure 8b. In black neon tetra, the focal fish decelerates when the neighbor is in front and at a distance of less than their body length; this effect is not so clear in zebrafish. As the figure shows, acceleration is symmetrical with respect to the horizontal axis, that is, it does not depend on the sign of the relative angle.

Acceleration and turning angle tend to be inversely related. The closer the turning angle of the focal fish to $\pm 90°$, the closer its acceleration is to zero, and the closer its turning angle is to zero,

This document is copyrighted by the American Psychological Association or one of its allied publishers.
This article is intended solely for the personal use of the individual user and is not to be disseminated broadly.

Table 1
Means and Standard Deviations of the Ratio of Mean Interindividual Distance to Mean Body Length (D) and Polarization (P), per Species and Group Size, and for the Aggregate of the Four Group Sizes

Global measures	Group size								Aggregate	
	2		3		4		8			
	M	*SD*	*M*	*SD*	*M*	*SD*	*M*	*SD*	*M*	*SD*
D ratio										
Neon	1.76	0.60	3.21	1.11	2.98	0.70	3.67	0.66	2.91	1.06
Zebrafish	1.75	0.49	3.56	4.26	3.62	2.65	4.54	2.96	3.36	3.07
Polarization										
Neon	.91	.06	.81	.11	.85	.06	.81	.07	.85	.09
Zebrafish	.77	.08	.68	.09	.52	.09	.52	.12	.62	.15

Note. Sample size is 60 per species and group (10 days, six video fragments per day), 480 for the aggregate.

the greater its acceleration (if its neighbor is in front) or deceleration (if its neighbor is behind). Figure 9 shows how average acceleration (s_a) and average turning angle (β_a) are related for several values of the relative angle from the focal fish to its neighbor (α_{ab}). As shown in Figures 5 and 7a, the average turning angle and average acceleration of the focal fish are functions of the sine and cosine of the relative angle. Therefore, the relationship between average turning angle and average acceleration is a parametric, ellipsoid function of the relative angle, as Figure 9 shows. A model that reasonably fits the average data is:

$$s_a = p \cdot \left(1 - \frac{1}{4}\frac{|\alpha_{ab}|}{180}\right) \cdot \cos\alpha_{ab}$$

$$\beta_a = q \cdot \sin\alpha_{ab}$$

with $p = 3.36$ cm/s^2, $q = 20.04$ degrees/s for black neon tetra and $p = 4.84$ cm/s^2, $q = 94.35$ degrees/s for zebrafish (maximum mean acceleration and positive turning angles in each species). In zebrafish, the ranges of accelerations and turning angles tend to be bigger than in black neon tetra. If all the fish in a group moved at a constant speed and did not change direction, the graph in Figure 9 would be reduced to a point at (0, 0). If they changed their velocities depending on the position of their neighbors but did not change direction, the graph would be reduced to a vertical line segment on the *y* axis; conversely, if they maintained their velocities but changed direction, it would be reduced to a line segment on the *x* axis. Therefore, an ellipsoid with a small horizontal axis indicates that the group shows high polarization, as is the case of black neon tetra, and an ellipsoid with big horizontal and vertical axes indicates that the group shows low polarization and frequent changes in velocity, as is the case of zebrafish. The graphs in Figure 9 may be useful for comparing the collective motion of different fish species and characterizing it either as highly polarized schools versus shoals or swarms.

Discussion

As found in previous studies, the global motion styles of groups of zebrafish and black neon tetra can be characterized as shoals and schools, respectively, according to the definitions in Pitcher and Parrish (1993). In general, as group size increases in both species, the mean interindividual distance increases and mean polarization decreases, although no remarkable differences regarding local interaction rules are found as a function of group size. However, big groups of black neon tetra tend to move more cohesively and polarized than big groups of zebrafish. In fact, as group size increases, the mean polarization of black neon tetra remains fairly stable, whereas it drops in zebrafish. High polarization values in black neon tetra at the macro level are a direct consequence of small heading differences between pairs of individuals at the micro level, an effect that is consistent across group size. In contrast, in zebrafish, greater variability in pairwise heading differences accounts for less polarization at the macro level, an effect that tends to increase as group size increases. In both species, a higher mean interindividual distance as group size increases partly explains the decrease in polarization, as individuals located far away from each other (three or more times their body length) do not tend to maintain small heading differences. In black neon tetra, as group size increases, relative angles between individuals tend to be uniformly distributed, meaning that there is no preferential relative position among individuals; in zebrafish, relative angles have a clear bimodal distribution, with fish showing a preference for swimming in front of or behind neighbors, not alongside them. Thus, relative positions in black neon tetra tend to be isotropic, whereas zebrafish tend to move along a line. In comparison, Herbert-Read et al. (2011) found that in mosquitofish, whose mean polarization is .84, .71, and .63 for groups of two, four, and eight fish, relative positions have a bimodal distribution like that of zebrafish, whereas their heading differences show little variability and are distributed like those of black neon tetra.

Turning angles are higher in zebrafish than in black neon tetra. The zebrafish preference for front and rear positions with respect to their neighbors explains the minimum turning angle in those cases, but the angle reaches a maximum (about 90°) when the neighbor is located to the side and the focal fish turns directly toward it. On the other hand, the lack of preference for relative positions in black neon tetra explains the smaller turning angles. However, in both species, the turning angle of the focal fish is big when the neighbor's heading is very different from its own, but not when its heading is very similar. Therefore, what causes the fish to turn toward their neighbors seems to be a sizable heading difference, and the turning angle is greater as that difference increases. This presumably makes the heading difference decrease, thus promoting group polarization.

This document is copyrighted by the American Psychological Association or one of its allied publishers.
This article is intended solely for the personal use of the individual user and is not to be disseminated broadly.

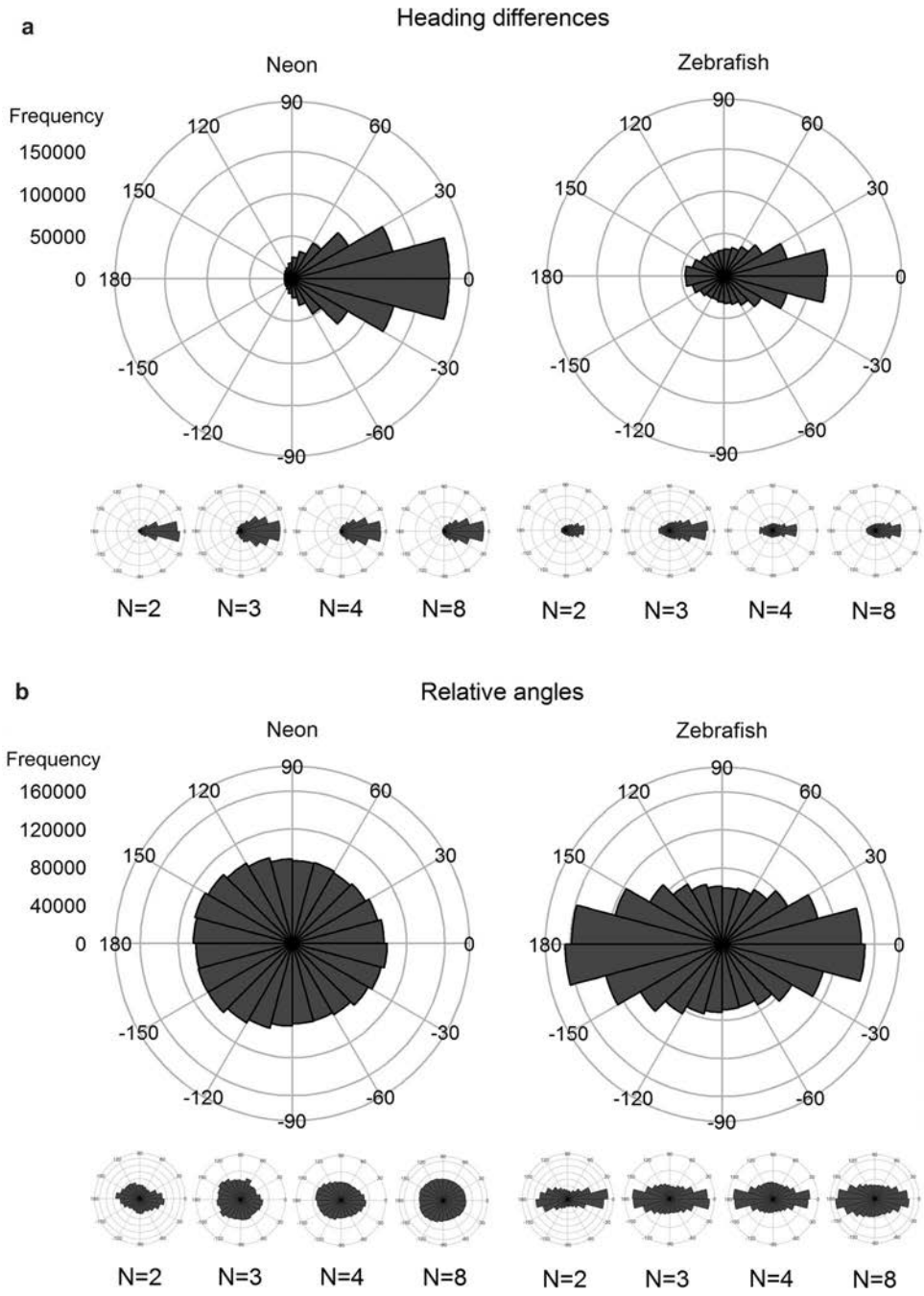


Figure 4. Circular histograms of a) heading differences (γ) and b) relative angles (α), per species and group size. Big graphs represent data pooled over all group sizes. In each video frame, the heading differences were computed for each pair of fish and aggregated for all pairs, while the relative angles were computed for each individual taken as focal and aggregated for all individuals. Thus, for group size N, the total sample size for a histogram of heading differences is $N(N-1)/2$ pairs $\times$ 500 frames $\times$ 6 fragments $\times$ 10 days $= 15{,}000 \times N(N-1)$, that is, 30,000 ($N = 2$), 90,000 ($N = 3$), 180,000 ($N = 4$), 840,000 ($N = 8$), and 1,140,000 (total). For a given group size, the total sample size for a histogram of relative angles is twice these values.

In black neon tetra, the turning angles toward the neighbor when the heading difference is maximum are bigger if the neighbor swims toward the focal fish than when it swims away from it; similar results were reported for mosquitofish by Herbert-Read et al. (2011) when the fish are at short distance from each other. The likely consequence of this is a momentary increase in the heading difference in the first case and a momentary decrease in the second. In zebrafish, this effect is not so evident. In both species,

This document is copyrighted by the American Psychological Association or one of its allied publishers.
This article is intended solely for the personal use of the individual user and is not to be disseminated broadly.

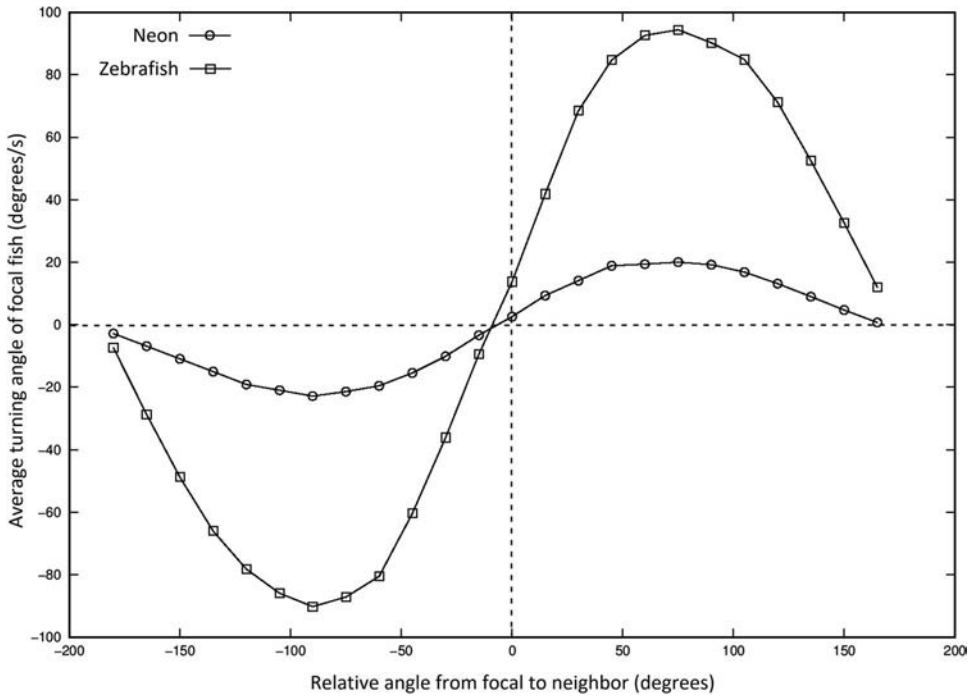


Figure 5. Average turning angle (β_a, degrees/s) of focal fish *A* as a function of its relative angle to its neighbor *B* (α_{ab}), per species. Data for group sizes 2, 3, 4, and 8 are pooled.

the greater the distance from the focal fish to its neighbor, the bigger the turning angle; thus, when a black neon tetra turns toward a neighbor swimming toward it at a certain distance, their heading difference momentarily increases but the distance between them decreases. Cohesion is thus the primary goal achieved at the expense of a temporary loss of polarization. Moreover, in black neon tetra, at a short distance (less than a body length), the focal fish tends to turn away from its neighbor and temporarily lose cohesion and polarization, a result found in mosquitofish (Herbert-Read et al., 2011) and golden shiners (Katz et al., 2011).

Therefore, avoiding excessive proximity (and eventual collision) takes priority over cohesion, and cohesion takes priority over polarization. This empirical result supports the rules proposed in Reynolds' (1987) general model of CCM and in models of fishes and birds' CCM (Couzin et al., 2002; Hemelrijk & Hildenbrandt, 2008; Hemelrijk & Kunz, 2005; Huth & Wissel, 1994), although other models consider attraction to be a priority over collision avoidance (Aoki, 1982). Such empirical conclusions about collision avoidance cannot be drawn from the zebrafish results; first, the turning angle toward a neighbor fish does not seem substantially different depending on whether the neighbor is swimming toward the focal fish or away from it, and zebrafish do not tend to lose polarization temporarily (which, in any case, tends to be low) at the expense of gaining cohesion; and, second, at a short distance, the turning angle is not reversed and the fish seem to tolerate excessive proximity. However, from visual inspection of the video recordings, it is evident that in many cases zebrafish cross their trajectories by swimming on top of each other so they do not need to avoid collision. This result is consistent with the observations of Spence et al. (2006), which indicate that zebrafish tend to be vertically distributed throughout the water column. Conversely, black neon tetra tend to swim in a particular stratum of the water column (Gimeno et al., 2016), and this causes them to turn away from neighbors when they are too close.

In both black neon tetra and zebrafish, fish tend to maintain their velocity when their relative angle to their neighbors is about 90°, that is, when they swim alongside each other, but they accelerate when their neighbors are in front and decelerate when they are behind at a rate that is greater in zebrafish than in black neon tetra, and greater when the neighbors are far away than when they are closer. Fish that are distant and facing each other (i.e., are in front of each other and antipolarized) tend to accelerate; this effect was found in both zebrafish and black neon tetra, and was also reported for mosquitofish by Herbert-Read et al. (2011). On the other hand, the focal fish tends to decelerate when its neighbors are behind it, polarized, and distant; this effect was found in black neon tetra. In the first case, acceleration promotes cohesion probably at the expense of temporarily maintaining low polarization; in the second case, deceleration promotes cohesion while maintaining polarization. In black neon tetra, when the neighbor is closer than one body length and in front of the focal fish, the latter decelerates, and when the former is behind, the focal fish accelerates. As with turning angle, this reversion has the effect of avoiding excessive proximity at the expense of momentarily losing cohesion and is analogous to what Herbert-Read et al. (2011) and Katz et al. (2011) reported for mosquitofish and golden shiners, respectively. Also, as with turning angle values, acceleration and deceleration values are independent of whether neighbors are located to the left or right of the focal fish.

This document is copyrighted by the American Psychological Association or one of its allied publishers.
This article is intended solely for the personal use of the individual user and is not to be disseminated broadly.

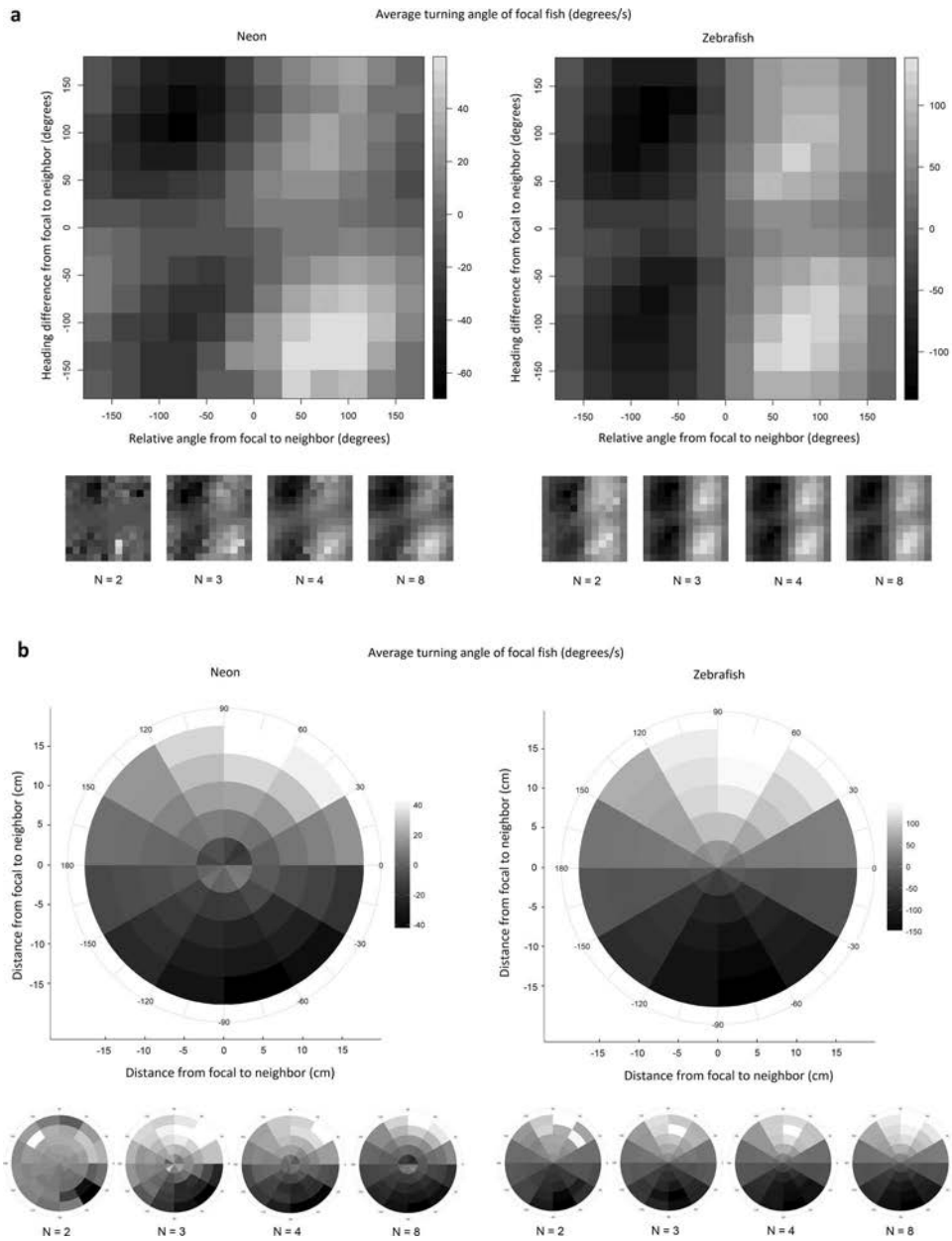


Figure 6. Heat maps of turning angles, per species and group size; big graphs represent data pooled over all group sizes. Note that the scales for the heat maps are different for the two species, with turning angles being generally bigger in zebrafish than in black neon tetra. a) Average turning angle (β_a, degrees/s) of focal fish *A* as a function of its relative angle (α_{ab}) and heading difference (γ_{ab}) to its neighbor *B*; light cells represent positive turns (left), dark cells represent negative turns (right). A positive relative angle means that the neighbor is on the left of the focal fish, a negative angle means that it is on the right; a null angle indicates the neighbor is in front, a ± 180 angle indicates that it is behind. Positive heading differences mean that the focal fish should turn left to align with its neighbors; negative differences mean it should turn right to align with them; a null difference indicates that they are completely polarized. b) Average turning angle of focal fish *A* as a function of its relative angle to its neighbor *B* and their distance (d_{ab}). The focal fish is located at the center of the figure facing in its direction of motion (to 0°); the areas above the horizontal represent areas lying to the left of the focal fish, and the ones below the horizontal represent areas lying to its right. A light cell indicates that the focal fish tends to turn left to any neighbor located in that cell, while a dark cell indicates that the focal fish tends to turn right to any neighbor located in it. The lighter the cell the greater is the left turn; the darker the cell the greater is the right turn. Therefore, as the figures show, the focal fish tends to turn left when its neighbors are at its left, and to turn right when they are at its right, and the more distant are the neighbors the greater are the turning angles.

This document is copyrighted by the American Psychological Association or one of its allied publishers.
This article is intended solely for the personal use of the individual user and is not to be disseminated broadly.

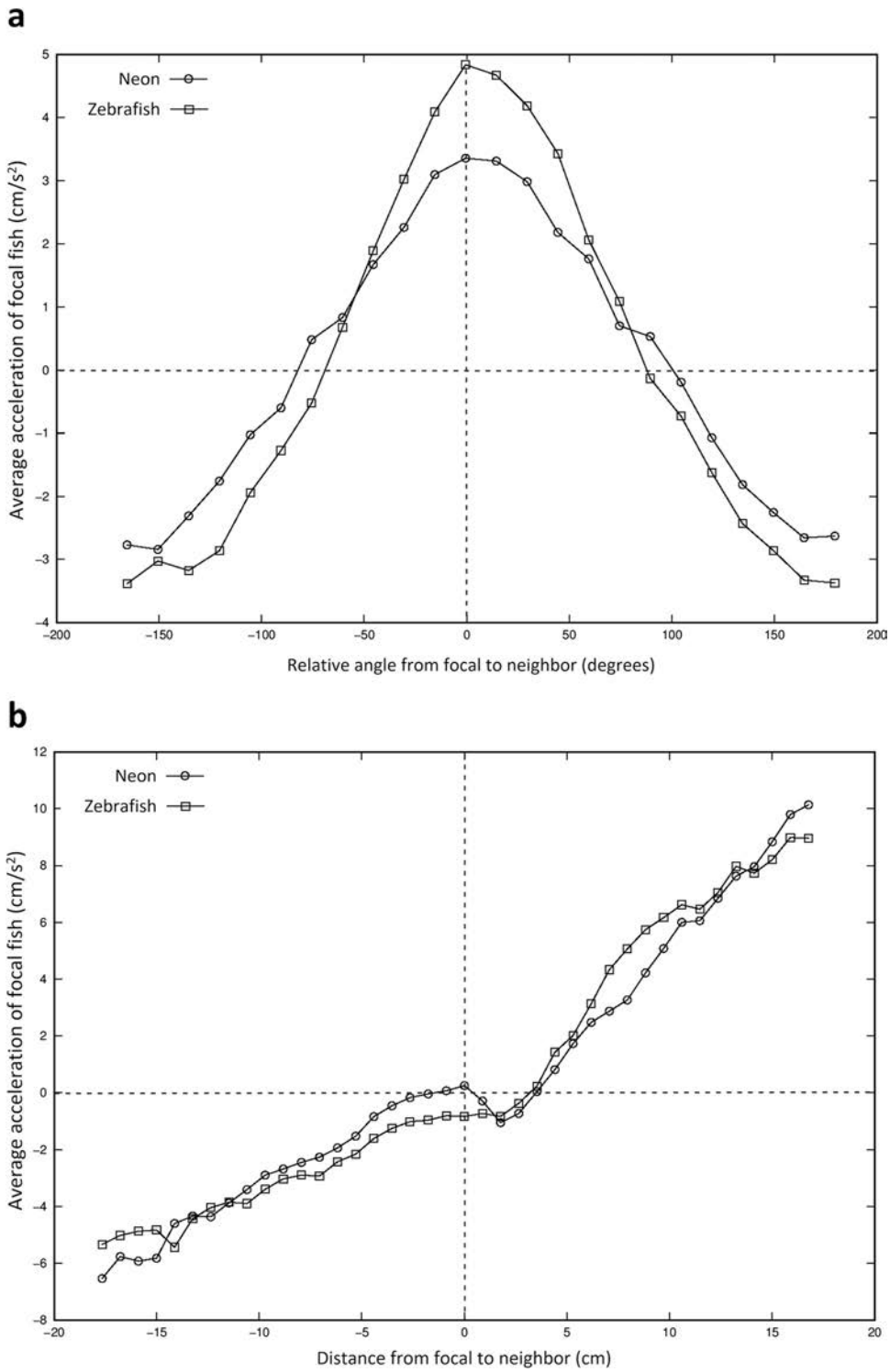


Figure 7. Average acceleration (s_a, cm/s^2) of focal fish *A* as a function of a) its relative angle (α_{ab}) and b) its distance (d_{ab}) to its neighbor *B*. Data for group sizes 2, 3, 4, and 8 are pooled.

We found that two features (global cohesion and polarization) that characterize collective motion in the two species of fish at the macro level can be explained by dyadic interaction rules based on individuals' changes in direction and velocity. From the relationships between these variables at the micro level, the kind of movement at the group level can be inferred. We have shown that the differences in cohesion and polarization between groups of black neon tetra (schools) and zebrafish (shoals) (Gimeno et al.,

This document is copyrighted by the American Psychological Association or one of its allied publishers.
This article is intended solely for the personal use of the individual user and is not to be disseminated broadly.

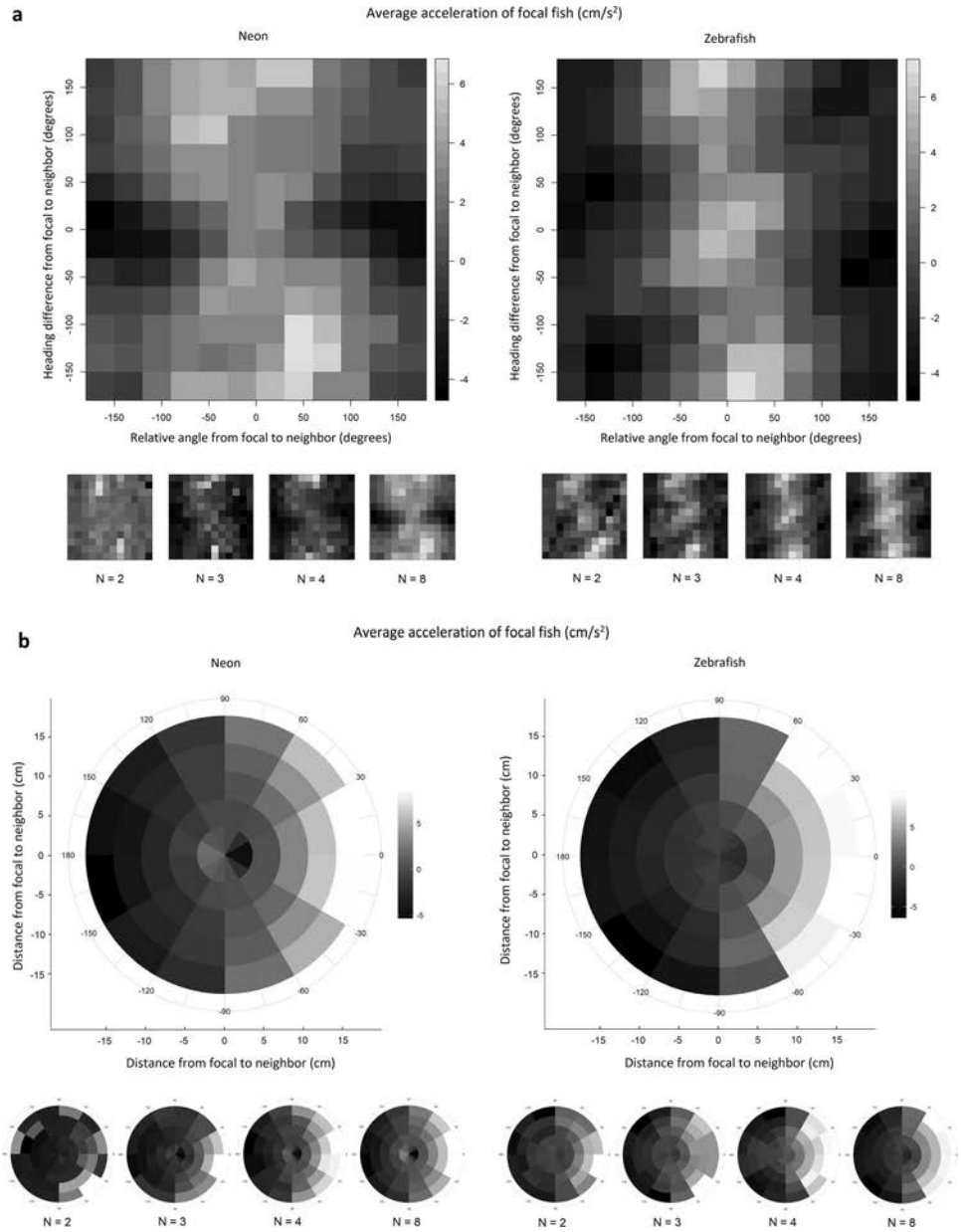


Figure 8. Heat maps of average acceleration, per species and group size; big graphs represent data pooled over all group sizes. a) Average acceleration (s_a, cm/s^2) of focal fish *A* as a function of its relative angle (α_{ab}) and heading difference (γ_{ab}) to its neighbor *B*; light cells represent positive acceleration, dark cells represent negative acceleration. b) Average acceleration of a focal fish as a function of its relative angle to its neighbor *B* and their distance (d_{ab}). The focal fish is located at the center of the figure facing in its direction of motion (to 0°); the areas above the horizontal represent areas lying to the left of the focal fish, and the ones below the horizontal represent areas lying to its right. A light cell indicates that the focal fish tends to accelerate when a neighbor is located in that cell, whereas a dark cell indicates that the focal fish tends to decelerate when a neighbor is located in it. The lighter the cell, the greater is the acceleration; the darker the cell, the greater is the deceleration. Therefore, as the figures show, the focal fish tends to accelerate more when its neighbors are in front of it and to decelerate more when they are behind it; in both species, the more distant are the neighbors in front or behind the focal fish, the greater is the acceleration or deceleration, respectively. However, when the neighbors are very close, focal black neon tetra tend to accelerate if the neighbors are behind it and to decelerate when they are in front of it.

This document is copyrighted by the American Psychological Association or one of its allied publishers.
This article is intended solely for the personal use of the individual user and is not to be disseminated broadly.

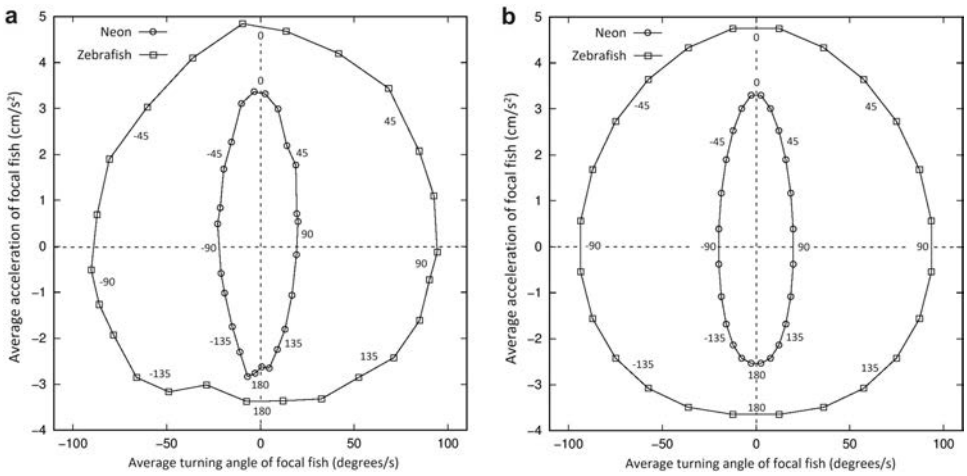


Figure 9. Relationship between average acceleration (s_a) and average turning angle (β_a), per species. a) Data pooled over all group sizes. Points in the graphs correspond to the relative angle of focal fish to their neighbors (α_{ab}), measured in degrees, as indicated in the graph. b) Model of s_a and β_a as parametric functions of α_{ab}; see text for explanation.

2016) are related to differences in the values of turning angles and accelerations and their relationships to relative angles and heading differences between pairs of individuals. The functions relating those variables are comparable with the ones found by Herbert-Read et al. (2011) in mosquitofish, a species whose collective motion (e.g., its polarization) appears to be halfway between zebrafish and black neon tetra. Like zebrafish, mosquitofish have a preference for swimming either in front or behind their neighbors rather than alongside; like black neon tetra, they have low variability of heading differences, that is, high polarization, "repulsion" zones at distances of less than one body length, and turning angles toward their neighbors that depend on both their heading difference and relative angle.

Although the universality of the interaction rules from which CCM emerges remains to be explored, there is evidence that the rules are similar in species from three distinct families, *Cyprinidae* (*Notemigonus* and *Danio*), *Poeciliidae* (*Gambusia*), and *Characidae* (*Hyphessobrycon*), and the differences might be a matter of degree (e.g., in turning angle, distance, and acceleration). Also, the existence of the rules studied in this and the aforementioned articles provides substantial empirical evidence to support the theoretical assumptions made in well-known classical agent-based models used to simulate collective coordinated motion in many different animal species, notably Reynolds (1987) and Huth and Wissel (1994).

References

Aoki, I. (1982). A simulation study on the schooling mechanism in fish. *Nippon Suisan Gakkaishi, 48,* 1081–1088. http://dx.doi.org/10.2331/suisan.48.1081

Buhl, J., Sumpter, D. J., Couzin, I. D., Hale, J. J., Despland, E., Miller, E. R., & Simpson, S. J. (2006). From disorder to order in marching locusts. *Science, 312,* 1402–1406. http://dx.doi.org/10.1126/science.1125142

Calovi, D. S., Lopez, U., Ngo, S., Sire, C., Chaté, H., & Theraulaz, G. (2014). Swarming, schooling, milling: Phase diagram of a data-driven fish school model. *New Journal of Physics, 16,* 015026. http://dx.doi.org/10.1088/1367-2630/16/1/015026

Couzin, I. D., James, R., Mawdsley, D., Croft, D. P., & Krause, J. (2006). Social organization and information transfer in schooling fishes. In C. Brown, K. Laland, & J. Krause (Eds.), *Fish cognition and behavior* (2nd ed., pp. 166–185). Oxford, United Kingdom: Wiley-Blackwell. http://dx.doi.org/10.1002/9780470996058.ch9

Couzin, I. D., Krause, J., James, R., Ruxton, G. D., & Franks, N. R. (2002). Collective memory and spatial sorting in animal groups. *Journal of Theoretical Biology, 218,* 1–11. http://dx.doi.org/10.1006/jtbi.2002.3065

Czirók, A., & Vicsek, T. (2000). Collective behavior of interacting self-propelled particles. *Physica A, 281,* 17–29. http://dx.doi.org/10.1016/S0378-4371(00)00013-3

Delcourt, J., Denoel, M., Ylieff, M., & Poncin, P. (2013). Video multitracking of fish behaviour: A synthesis and future perspectives. *Fish and Fisheries, 14,* 186–204. http://dx.doi.org/10.1111/j.1467-2979.2012.00462.x

Delcourt, J., & Poncin, P. (2013). Shoals and schools: Back to the heuristic definitions and quantitative references. *Reviews in Fish Biology and Fisheries, 22,* 595–619. http://dx.doi.org/10.1007/s11160-012-9260-z

Deneubourg, J. L., & Goss, S. (1989). Collective patterns and decision-making. *Ethology Ecology and Evolution, 1,* 295–311. http://dx.doi.org/10.1080/08927014.1989.9525500

Dolado, R., Gimeno, E., Beltran, F. S., Quera, V., & Pertusa, J. F. (2015). A method for resolving occlusions when multitracking individuals in a shoal. *Behavior Research Methods, 47,* 1032–1043. http://dx.doi.org/10.3758/s13428-014-0520-9

Emlen, J. Y., Jr. (1952). Flocking behavior in birds. *The Auk, 69,* 160–170. http://dx.doi.org/10.2307/4081266

Gimeno, E., Quera, V., Beltran, F. S., & Dolado, R. (2016). Differences in shoaling behavior in two species of freshwater fish (*Danio rerio* and *Hyphessobrycon herbertaxelrodi*). *Journal of Comparative Psychology, 130,* 358–368. http://dx.doi.org/10.1037/com0000041

Gueron, S., Levin, S. A., & Rubenstein, D. I. (1996). The dynamics of herds: From individuals to aggregations. *Journal of Theoretical Biology, 182,* 85–98. http://dx.doi.org/10.1006/jtbi.1996.0144

Helbing, D., Molnár, P., Farkas, I. J., & Bolay, K. (2001). Self-organizing pedestrian movement. *Environment and Planning B, 28,* 361–383. http://dx.doi.org/10.1068/b2697

Hemelrijk, C. K., & Hildenbrandt, H. (2008). Self-organized shape and frontal density of fish schools. *Ethology, 114,* 245–254. http://dx.doi.org/10.1111/j.1439-0310.2007.01459.x

This document is copyrighted by the American Psychological Association or one of its allied publishers.
This article is intended solely for the personal use of the individual user and is not to be disseminated broadly.

Hemelrijk, C. K., & Kunz, H. (2005). Density distribution and size sorting in fish schools: An individual-based model. *Behavioral Ecology, 16,* 178–187. http://dx.doi.org/10.1093/beheco/arh149

Herbert-Read, J. E., Perna, A., Mann, R. P., Schaerf, T. M., Sumpter, D. J. T., & Ward, A. J. W. (2011). Inferring the rules of interaction of shoaling fish. *Proceedings of the National Academy of Sciences of the United States of America, 108,* 18726–18731. http://dx.doi.org/10.1073/pnas.1109355108

Huth, A., & Wissel, C. (1994). The simulation of fish schools in comparison with experimental data. *Ecological Modelling, 75/76,* 135–146. http://dx.doi.org/10.1016/0304-3800(94)90013-2

Katz, Y., Tunstrøm, K., Ioannou, C. C., Huepe, C., & Couzin, I. D. (2011). Inferring the structure and dynamics of interactions in schooling fish. *Proceedings of the National Academy of Sciences of the United States of America, 108,* 18720–18725. http://dx.doi.org/10.1073/pnas.1107583108

King, A. J., & Sueur, C. (2011). Where next? Group coordination and collective decision making by primates. *International Journal of Primatology, 32,* 1245–1267. http://dx.doi.org/10.1007/s10764-011-9526-7

Kunz, H., & Hemelrijk, C. K. (2003). Artificial fish schools: Collective effects of school size, body size, and body form. *Artificial Life, 9,* 237–253. http://dx.doi.org/10.1162/106454603322392451

Lee, A. (2013). VirtualDub (Version 1.19.11) [Computer software]. Retrieved from http://www.virtualdub.org

Leem, J. B., Jeon, W., Yun, C. Y., & Lee, S. H. (2012). Quantitative analysis of fish schooling behavior with different numbers of medaka (*Oryzias latipes*) and goldfish (*Carassius auratus*). *Ocean Science Journal, 47,* 445–451. http://dx.doi.org/10.1007/s12601-012-0040-4

Media Cybernetics, Inc. (2015). Image-Pro Premier (Version 9.1) [Computer software]. Bethesda, MD: Media Cybernetics, Inc.

Miller, N., & Gerlai, R. (2012a). Automated tracking of zebrafish shoals and the analysis of shoaling behavior. In A. V. Kalueff & A. M. Stewart (Eds.), *Zebrafish protocols for neurobehavioral research* (pp. 217–230). New York, NY: Humana Press. http://dx.doi.org/10.1007/978-1-61779-597-8_16

Miller, N., & Gerlai, R. (2012b). From schooling to shoaling: Patterns of collective motion in zebrafish (*Danio rerio*). *PLoS ONE, 7,* e48865. http://dx.doi.org/10.1371/journal.pone.0048865

Nagy, M., Ákos, Z., Biro, D., & Vicsek, T. (2010). Hierarchical group dynamics in pigeon flocks. *Nature, 464,* 890–893. http://dx.doi.org/10.1038/nature08891

Perna, A., Grégoire, G., & Mann, R. P. (2014). On the duality between interaction responses and mutual positions in flocking and schooling. *Movement Ecology, 2,* 22. http://dx.doi.org/10.1186/s40462-014-0022-5

Pitcher, T. J., & Parrish, J. (1993). Functions of shoaling behaviour in teleosts. In T. J. Pitcher (Ed.), *Behaviour of teleost fishes* (pp. 363–337). London, United Kingdom: Chapman & Hall/CRC. http://dx.doi.org/10.1007/978-94-011-1578-0_12

Quera, V., Beltran, F. S., & Gimeno, E. (2016). Modelling the emergence of coordinated collective motion by minimizing dissatisfaction. *Mathematical Biosciences, 271,* 154–167. http://dx.doi.org/10.1016/j.mbs.2015.11.007

Radakov, D. V. (1973). *Schooling in the ecology of fish*. New York, NY: Halsted Press.

Rasband, W. (2014). ImageJ (Version 1.48v) [Computer software]. Retrieved from http://imagej.nih.gov/ij/

R Development Core Team. (2014). R: A Language and Environment for Statistical Computing (Version 3.1.4) [Computer software]. Retrieved from http://www.R-project.org

Reynolds, C. W. (1987). Flocks, herds, and schools: A distributed behavioral model. *Computer Graphics, 21,* 25–34. http://dx.doi.org/10.1145/37402.37406

Rosenthal, S. B., Twomey, C. R., Hartnett, A. T., Wu, H. S., & Couzin, I. D. (2015). Revealing the hidden networks of interaction in mobile animal groups allows prediction of complex behavioral contagion. *Proceedings of the National Academy of Sciences of the United States of America, 112,* 4690–4695. http://dx.doi.org/10.1073/pnas.1420068112

Shelton, D. S., Price, B. C., Ocasio, K. M., & Martins, E. P. (2015). Density and group size influence shoal cohesion, but not coordination in zebrafish (*Danio rerio*). *Journal of Comparative Psychology, 129,* 72–77. http://dx.doi.org/10.1037/a0038382

Soria, M., Fréon, P., & Chabanet, P. (2007). Schooling properties of an obligate and a facultative fish species. *Journal of Fish Biology, 71,* 1257–1269. http://dx.doi.org/10.1111/j.1095-8649.2007.01554.x

Spence, R., Fatema, M. K., Reichard, M., Huq, K. A., Wahab, M. A., Ahmed, Z. F., & Smith, C. (2006). The distribution and habitat preferences of the zebrafish in Bangladesh. *Journal of Fish Biology, 69,* 1435–1448. http://dx.doi.org/10.1111/j.1095-8649.2006.01206.x

Strömbom, D. (2011). Collective motion from local attraction. *Journal of Theoretical Biology, 283,* 145–151. http://dx.doi.org/10.1016/j.jtbi.2011.05.019

Vicsek, T., & Zafeiris, A. (2012). Collective motion. *Physics Reports, 517,* 71–140. http://dx.doi.org/10.1016/j.physrep.2012.03.004

Received September 4, 2018
Revision received January 7, 2019
Accepted January 8, 2019 ■

This document is copyrighted by the American Psychological Association or one of its allied publishers.
This article is intended solely for the personal use of the individual user and is not to be disseminated broadly.